Electronic Supplementary Material (ESI) for Physical Chemistry Chemical Physics.

Supporting information

Computational Details

The chemical potential of each absorbed intermediate μ(*Int) at the electrochemical equilibrium condition is calculated using the following equation:

$$\mu(*Int) = E_{elec} + ZPE + \int C_p dT - TS + G_{solv}$$

$$\mu[X(aq)] = E_{elec} + ZPE + \int C_p dT - TS$$

(1). ZPE denotes the zero-point energy. The ZPE of the chemical-adsorbed species of all models are approximated using Ru-4N2v-CNT(5,5) model with the site density at 1/8. For the species in the solution phase, including CH_2O, CH_3OH, CH_4, CO, CO_2, H_2, H_2O and HCOOH, the values of ZPE reported in Ref. (a) are adapted and also tabulated in the computational details section of ESI.

(2). All of the integrals of $C_p dT$ (the enthalpy thermal correction) adapte the results reported by Ref. (a) and (b). These terms are relatively small and at the magnitude of 0.1 eV.

(3). TS denotes the entropy thermal correction. We approximate the TS of the chemical-adsorbed species of all models using Ru-4N2v-CNT(5,5) model with the site density at 1/8. We adapte the values of TS from Ref. (a) for the species in the solution phase where the TS terms of Ref. (a) contain the fugacity correction - $RT * ln(p/p_0)$. By doing so, we assume the same Faraday yield for the products of CO_2 electrochemical reduction using TM-4N2v-CNT models as that being observed on Cu surface by Hori et al. in Ref. (c). Therefore, the partial pressure of HCOOH in this study is assumed to be 2 Pa. It should be noted that the further revision for the TS terms could be important if the experimental Faraday field using TM-4N2v-CNT type of catalysts are available.

(4). G_{solv} denotes the solvation energy correction at -0.30 eV for all of the chemical-adsorbed species containing OH group.

(5). E_{elec} of CO(aq) on is corrected by +0.24 eV due to the use of PBE functional as suggested by Ref (d). E_{elec} of other models are directly obtained from the PBE calculations.

(6). References: (a) A. A. Peterson, F. Abild-Pedersen, F. Studt, J. Rossmeisl and J. K. Nørskov, *Energy Environ. Sci.*, 2010, 3, 1311-1315. (b) P. Hisunsit, *J. Phys. Chem. C* 2013, 117, 8262-8268. (c) Y. Hori, A. Murata and R. Takahashi, *J. Chem. Soc. Faraday T. 1,* 1989, 85, 2309-2326. (d) F. Calle-Vallejo and M. T. M. Koper, *Angew. Chem. Int. Ed.* 2013, 52, 7282-7285.

Numerical values of the correction terms (eV)			
Chemical-adsorbed Intermediates	ZPE	$\int C_p dT$	TS
*COOH	0.722	0.096	-0.112
*OCHO	0.681	0.102	-0.103
*COHOH	0.988	0.096	-0.169
*CO	0.156	0.076	-0.009
*CHO	0.546	0.086	-0.063
*COH	0.542	0.068	-0.112

*CH_2O	0.829	0.091	-0.153
*CHOH	0.880	0.068	-0.158
*OCH_3	1.161	0.093	-0.179
*CH_2OH	1.170	0.093	-0.106
*CH	0.370	0.028	-0.084
*CH_2	0.686	0.049	-0.100
*CH_3	0.994	0.060	-0.102
*H	0.200	0.005	-0.024
Non-adsorbed Intermediates	ZPE	$\int C_p dT$	[a]TS
CH_2O	0.700	0.100	-0.660
CH_3OH	1.350	0.110	-0.790
CH_4	1.200	0.100	-0.600
CO	0.140	0.090	-0.670
CO_2	0.310	0.100	-0.650
H_2	0.270	0.090	-0.420
H_2O	0.580	0.100	-0.650
HCOOH	0.900	0.110	-1.020

a. TS contains $RT \cdot ln(p/p_0)$ correction.

k-point configurations:

The following k-point configurations are used for the simulations at ρ_s = 1/3 ~ 1/8

ρ_s = 1/m	1/3	1/4	1/5	1/6	1/7	1/8
k-point	1*1*10	1*1*8	1*1*6	1*1*4	1*1*3	1*1*3

Table S1. The predicted N-Ru-N angle (θ_{NRuN}, degree) and N-Ru bond length (r_{RuN}, Å) of Ru-4N2v-CNT models												
CNT	(5, 5)		(6, 6)		(7, 7)		(8, 8)		(10, 10)		(12, 12)	
ρ_s	θ_{NRuN}	r_{RuN}	θ_{NRuN}	r_{RuN}	θ_{NRuN}	r_{RuN}	θ_{NRuN}	r_{RuN}	θ_{NRuN}	r_{RuN}	θ_{NRuN}	r_{RuN}
1/3	151.51°	1.96	153.92°	1.95	155.60°	1.95	156.99°	1.95	159.24°	1.95	159.81°	1.95
1/4	152.39°	1.95	154.96°	1.95	156.93°	1.94	158.16°	1.95	160.30°	1.95	161.77°	1.95
1/5	153.15°	1.95	155.60°	1.95	157.31°	1.95	159.02°	1.95	160.89°	1.95	163.23°	1.95
1/6	152.77°	1.96	155.28°	1.96	157.16°	1.96	158.58°	1.95	160.80°	1.95	162.56°	1.95
1/7	152.99°	1.96	155.54°	1.95	157.21°	1.95	158.87°	1.96	160.97°	1.96	162.05°	1.96
1/8	153.26°	1.97	155.65°	1.96	157.71°	1.96	159.05°	1.96	159.95°	1.96	162.63°	1.96
Avg.	152.68°	1.96	155.16°	1.95	156.99°	1.95	158.45°	1.95	160.36°	1.95	162.01°	1.95

■ θ_{NRuN} is the average angle of N_1-TM-N_2 where N_1 and N_2 are the nitrogen substitutions across each other.

Table S2. The calculated d-band center of Ru-4N2V-CNT models.

ρ_s	(5,5) d-center	(6,6) d-center	(7,7) d-center	(8,8) d-center	(10,10) d-center	(12,12) d-center
1/3	-0.69	-0.65	-0.61	-0.42	-0.32	-0.35
1/4	-0.52	-0.69	-0.60	-0.41	-0.45	-0.51
1/5	-0.68	-0.61	-0.59	-0.58	-0.60	-0.27
1/6	-0.57	-0.63	-0.76	-0.67	-0.40	-0.42
1/7	-0.41	-0.32	-0.60	-0.62	-0.48	-0.43
1/8	-0.51	-0.38	-0.57	-0.30	-0.21	-0.28
Avg.	-0.57	-0.54	-0.62	-0.50	-0.41	-0.38

Table. S3. ΔE_{TM} , r_{NM} , θ_{NMN} and d-band center in various TM-4N2V-CNT models at $\rho_S = 1/8$.[1]

TM		Fe	Ru	Os	Co	Rh	Ir	Ni	Pt	Cu
Atomic radius (Å)		1.17	1.25	1.26	1.16	1.25	1.27	1.15	1.30	1.17
Multi.	(5,5)	2	2	2	1	1	1	0	0	1
	(12,12)	2	2	2	1	1	1	0	0	1
ΔE_{TM}	(5,5)	-1.93	-0.13	0.69	-1.14	-0.16	-0.42	-2.86	-3.36	-1.35
	(12,12)	-2.64	-0.57	0.29	-1.82	-1.02	-1.02	-3.44	-4.03	-1.90
	[2]GR	-2.52	-0.34	0.35	-1.99	-1.63	-1.25	-3.09	-2.32	-1.66
r_{NM}	(5,5)	1.88	1.97	1.96	1.85	1.95	1.95	1.85	1.96	1.90
	(12,12)	1.88	1.96	1.95	1.86	1.94	1.94	1.85	1.95	1.91
	diff.	0.00	0.01	0.01	-0.01	0.01	0.00	0.00	0.01	-0.01
θ_{NMN}	(5,5)	170.57°	153.26°	155.57°	167.66°	163.10°	164.72°	173.37°	170.41°	174.25°
	(12,12)	179.47°	162.63°	164.93°	174.24°	173.17°	173.13°	179.98°	177.36°	179.60°
	diff.	8.89°	9.37°	9.36°	6.58°	10.06°	8.40°	6.61°	6.95°	5.35°
d-band center[3]	(5,5)	-0.99	-0.51	-0.60	-0.46	-0.76	-0.79	-1.49	-2.44	-3.32
	(12,12)	-0.88	-0.28	-0.29	-0.66	-0.41	-0.82	-1.56	-2.33	-3.12
	diff.	0.11	0.23	0.31	0.20	0.35	0.03	0.07	0.12	0.20

1. ΔE_{emb} is in eV, r_{NM} is in Å and θ_{NMN} is in degree.
2. GR denotes ΔE_{TM} predicted by the 4N2v-graphene models in Ref 79.
3. The schematic representations of partial density of state (PDOS) are summarized in Figure S5.

Table S4. Adsorption energy in eV of CO_2, CO and H_2O on Ru-4N2V-CNT models.

Adsorbate / (n, n)	CO_2	CO	H_2O[1]
(5,5)	-0.56	-1.84	-
(6,6)	-0.58	-1.91	-
(7,7)	-0.76	-2.27	-
(8,8)	-0.79	-2.21	-0.18
(10,10)	-0.82	-2.30	-0.21
(12,12)	-0.87	-2.37	-0.27

1. The absence of adsorption energy denotes that H_2O binding is repulsive.

Table S5. The formation energy (in eV) of possible intermediates for CO_2RR.

# of e^-+H^+	(1) * + CO_2(aq) + 0.5H_2(aq) →			(2) * + CO_2(aq) + H_2(aq) →		
	*H + CO_2(aq)	*C(=O)OH	*OCH(=O)	*C(OH)OH	[3]CO + H_2O(aq)	*HC(=O)OH(aq)[1]
Fe	0.271	**0.421**	0.872	0.770	**-0.276**	0.268
Ru	-0.206	**-0.072**	0.880	0.176	**-0.835**	0.268
Os	-0.365	**-0.228**	0.757	-0.105	**-1.148**	0.268
Co	0.314	**0.555**	1.305	1.522	0.374	**0.268**
Rh	0.077	**0.405**	1.559	1.635	0.374	**0.268**
Ir	-0.172	**0.154**	1.516	1.225	0.293	**0.268**
Ni	1.839	**2.027**	2.126	2.521	0.374	**0.268**
Pt	1.579	**2.033**	2.477	2.614	0.374	**0.268**
Cu	1.960	2.071	**1.945**	2.224	0.374	**0.268**
Ru_12	-0.514	**-0.293**	0.564	-0.140	**-1.163**	0.268
Ru_G	-0.138	**-0.265**	0.357	-0.310	**-1.360**	0.268
Rh_12	0.073	**0.465**	1.577	1.482	0.374	**0.268**
Rh_G	0.149	**0.143**	1.186	1.480	0.374	**0.268**

(1). All *HC(=O)OH intermediates are nearly desorbed from the metal binding site.

(2). The bold denotes the favorable formation of intermediate at each electrochemical step.

(3). *CO are used for the cases of $\Delta G < 0$ while others use CO(aq) (0.374 eV) for the formation energy.

Table S6. Calculated potentials for the CO_2RR, main product and potential-determining step (PDS).

TM	[1]Main product	[2]Potential (V)	PDS
Fe	*CO	-0.421	CO_2(g) → *COOH
Ru	*CO	> 0	
Os	*CO	> 0	
Co	HCOOH	-0.555	CO_2(g) → *COOH
Rh	HCOOH	-0.405	CO_2(g) → *COOH
Ir	HCOOH	-0.154	*COOH → HCOOH
Ni	HCOOH	-2.027	CO_2(g) → *COOH
Pt	HCOOH	-2.033	CO_2(g) → *COOH
Cu	HCOOH	-1.945	CO_2(g) → *OCHO
Ru_12	*CO	> 0	
Ru_G	*CO	> 0	
Rh_12	HCOOH	-0.465	CO_2(g) → *COOH
Rh_G	HCOOH	-0.143	*COOH → HCOOH

1. *CO could continuously undergo CORR mechanism as shown in Tables S6-S7.
2. For CO_2(aq) + 1/2H_2 → HCOOH(aq), ΔG = 0.547 eV.

Table S7. The formation energy (in eV) of possible intermediates for CORR

# of e^-+H^+	(I) $CO(aq) + 0.5H_2(aq) \rightarrow$		(II) $CO(aq) + H_2(aq) \rightarrow$		(III) $CO(aq) + 1.5H_2(aq) \rightarrow$		
	*CHO	*COH	$*CH_2O$ to desorb	*CHOH	$*OCH_3$	$*CH_2OH$	$*CH + H_2O$
Fe	**0.092**	1.116	0.132	**0.040**	0.000	**-0.007**	1.592
Ru	**-0.408**	0.530	0.132	**-0.624**	-0.103	**-0.327**	0.554
Os	**-0.573**	-0.175	0.132	**-0.964**	-0.357	**-0.498**	-0.376
Co	**0.137**	1.576	**0.132**	1.062	0.645	0.037	2.698
Rh	**0.008**	1.457	**0.132**	1.050	0.876	-0.101	2.397
Ir	**-0.235**	1.191	**0.132**	0.503	0.736	-0.244	1.817
Ni	**1.692**	2.979	**0.132**	2.479	1.577	1.366	4.576
Pt	**1.703**	3.305	**0.132**	2.636	1.909	1.297	4.175
Cu	**1.907**	2.980	**0.132**	2.089	1.613	1.492	4.357
Ru_12	**-0.544**	-0.037	0.132	**-0.861**	-0.322	**-0.591**	0.026
Ru_G	**-0.479**	0.080	0.132	**-0.982**	-0.499	**-0.659**	0.525
Rh_12	**0.146**	1.699	**0.132**	0.917	0.925	-0.007	2.610
Rh_G	**-0.151**	1.425	**0.132**	1.050	0.550	-0.291	2.485

# of e^-+H^+	(IV) $CO(aq) + 2H_2(aq) \rightarrow$			(V) $CO(aq) + 2.5H_2(aq) \rightarrow$	(VI) $CO(aq) + 3H_2(aq) \rightarrow$		
	$*O + CH_4(g)$	$CH_3OH(aq)$	$*CH_2 + H_2O$	$*CH_3 + H^2O$	$* + CH_4 + H_2O$	*CO	
Fe	-0.296	**-0.497**	0.295	-0.690	-1.587	-0.649	
Ru	-0.674	-0.497	**-0.575**	**-1.090**	**-1.587**	-1.209	
Os	-1.502	-0.497	**-1.087**	**-1.310**	**-1.587**	-1.521	
Co	1.109	-0.497	1.286	-0.614	-1.587	> 0	
Rh	1.282	-0.497	1.084	-0.768	-1.587	> 0	
Ir	0.766	-0.497	0.644	-0.960	-1.587	-0.081	
Ni	2.678	-0.497	2.810	0.800	-1.587	> 0	
Pt	2.930	-0.497	2.686	0.687	-1.587	> 0	
Cu	2.625	-0.497	2.696	0.858	-1.587	> 0	
Ru_12	-0.874	-0.497	**-0.813**	**-1.387**	**-1.587**	-1.537	
Ru_G	1.898	-0.497	**-0.742**	**-1.285**	**-1.587**	-1.734	
Rh_12	1.378	-0.497	1.118	-0.724	-1.587	> 0	
Rh_G	2.948	-0.497	1.019	-0.860	-1.587	> 0	

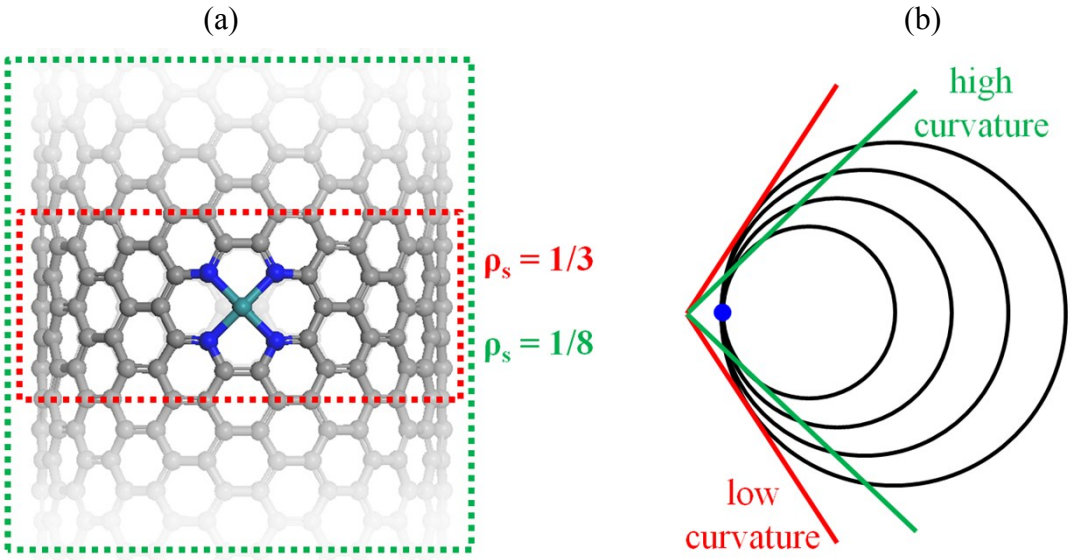

Figure S1. The schematic representation of (a) site density, denoted as $\rho_s = 1/m$ in which m is the number of unit cells of CNT for repeating TM, and (b) curvature of CNT.

Ru-4N2v-CNT(5,5)

1/3

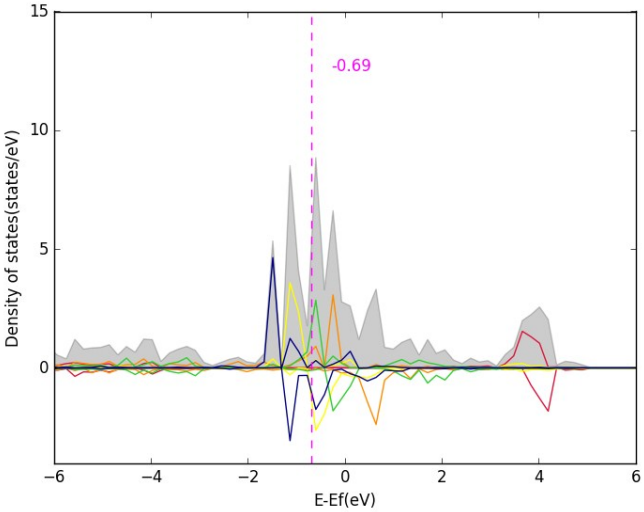

1/4

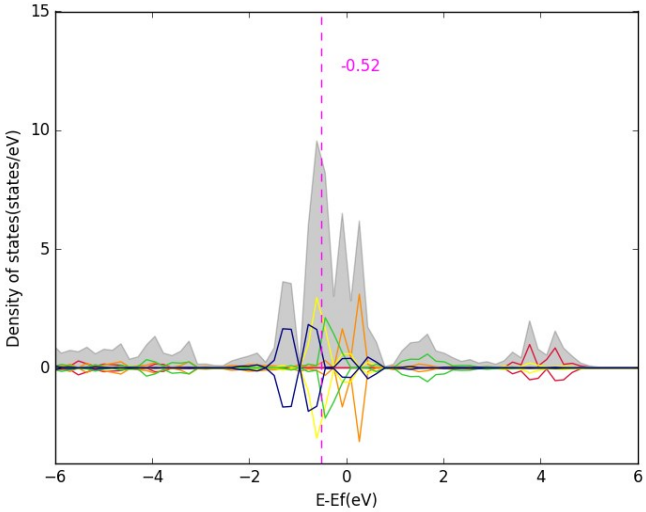

1/5

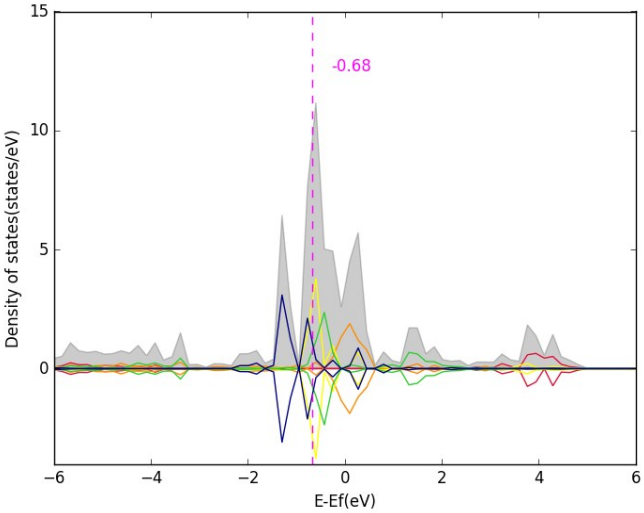

1/6

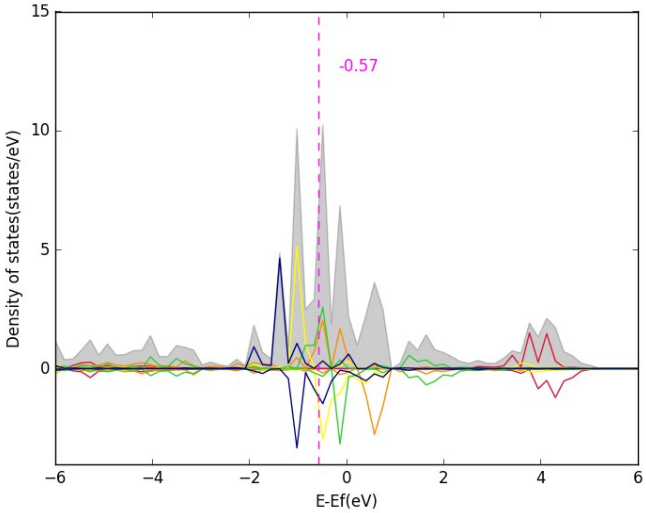

1/7

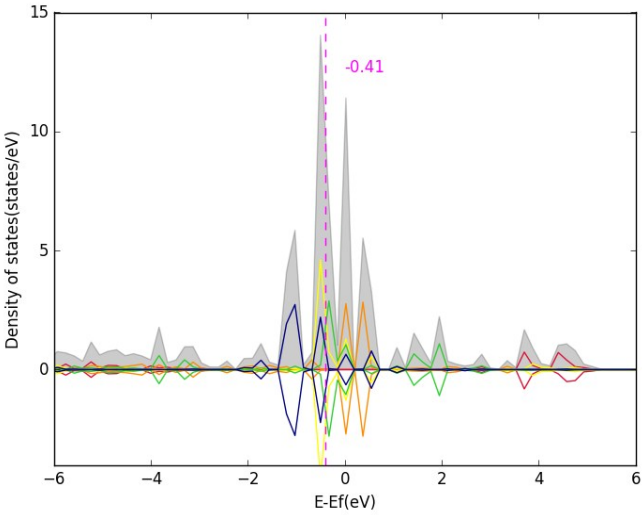

1/8

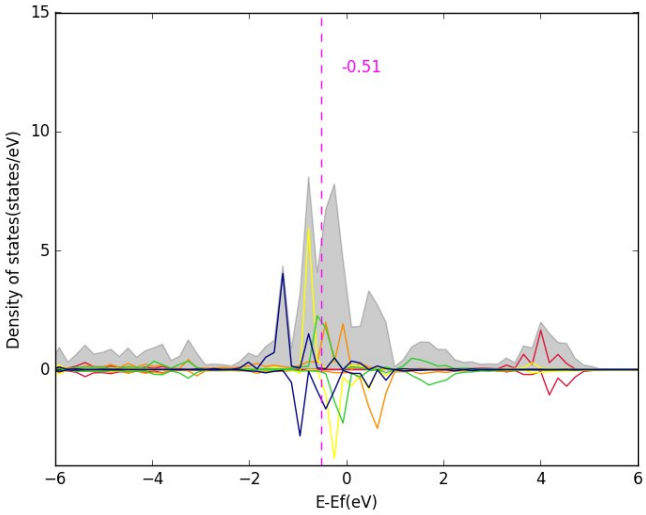

Ru-4N2v-CNT(6,6)

1/3

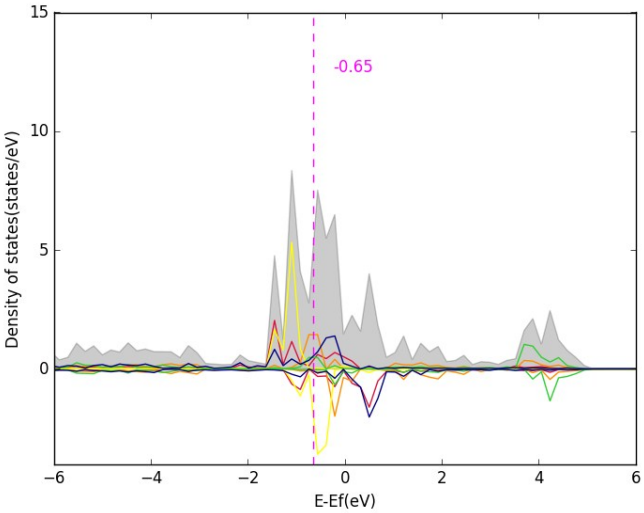

1/4

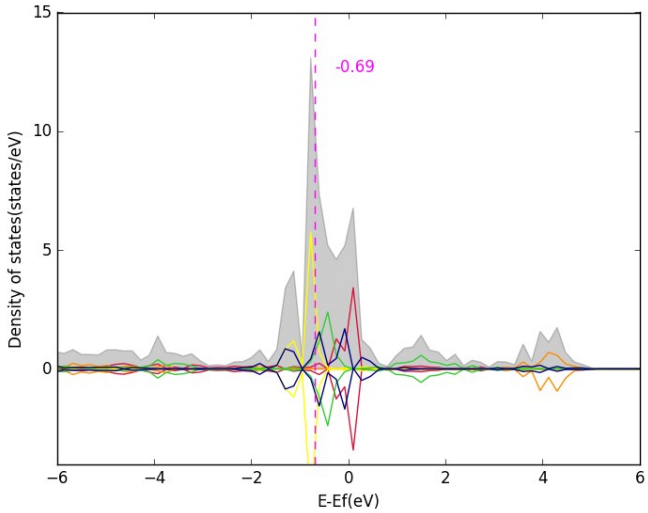

1/5

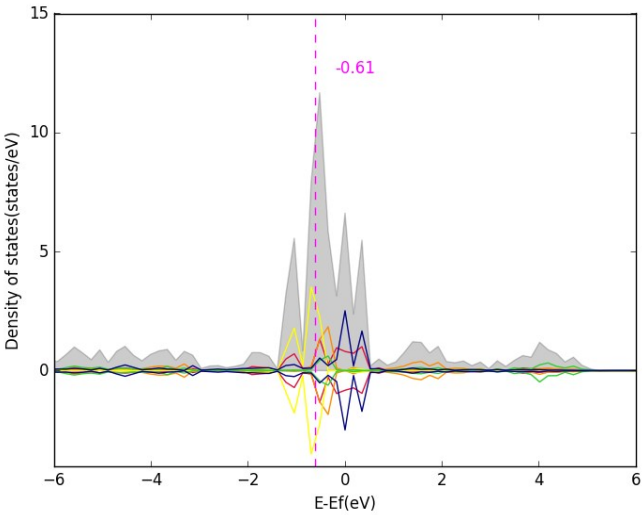

1/6

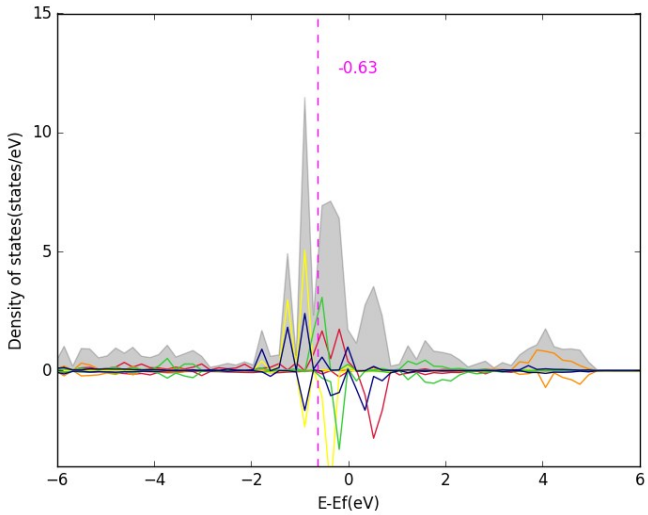

1/7

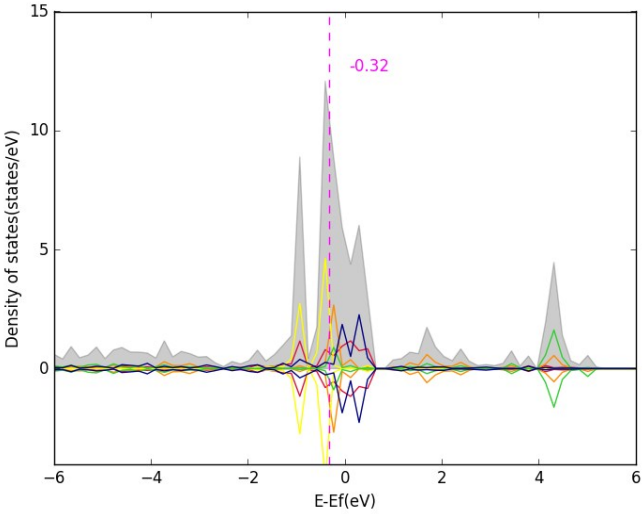

1/8

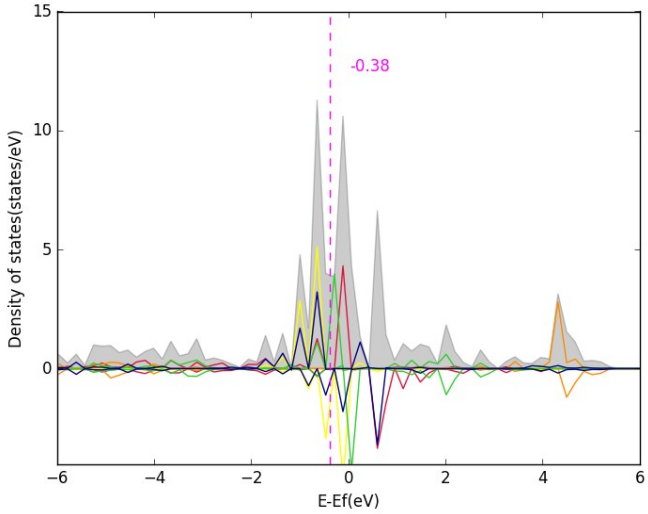

Ru-4N2v-CNT(7,7)

1/3

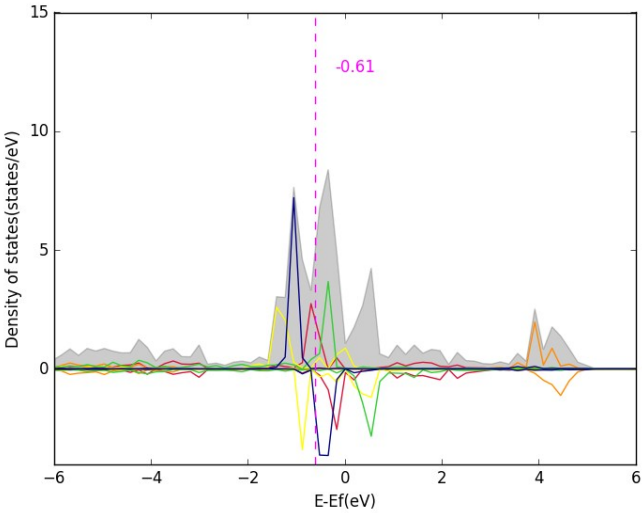

1/4

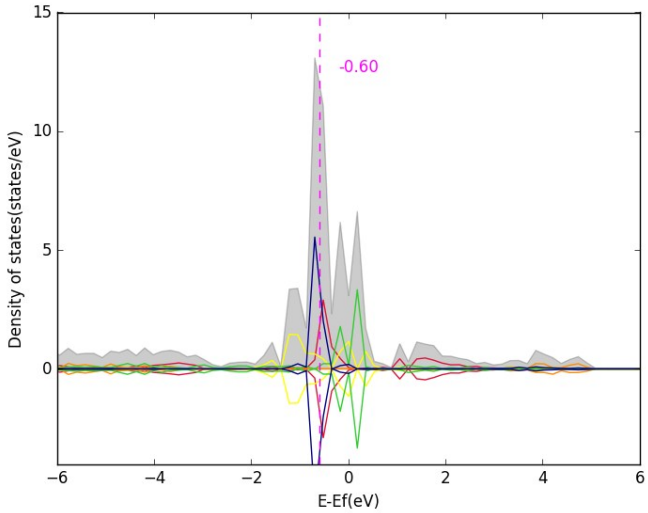

1/5

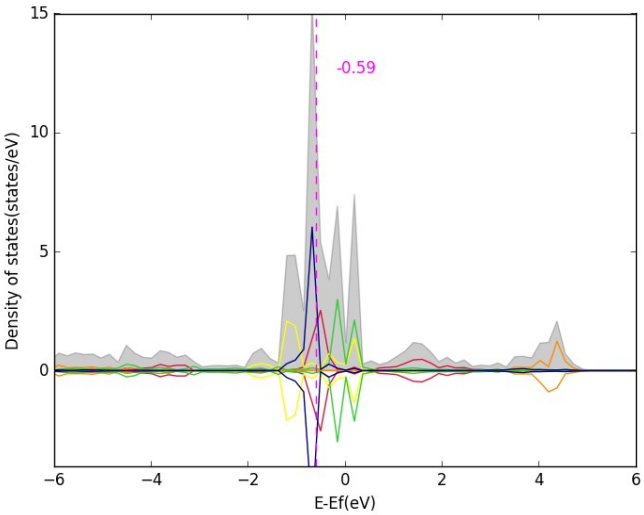

1/6

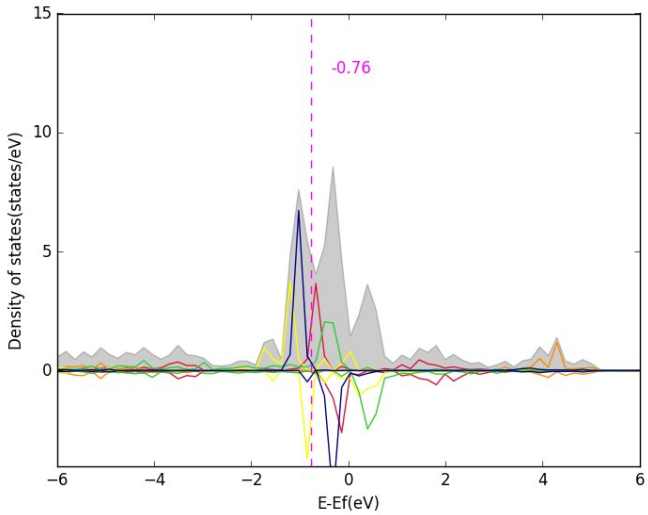

1/7

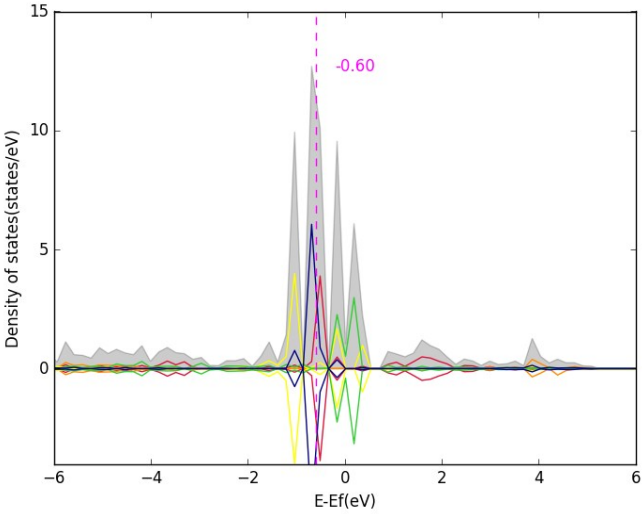

1/8

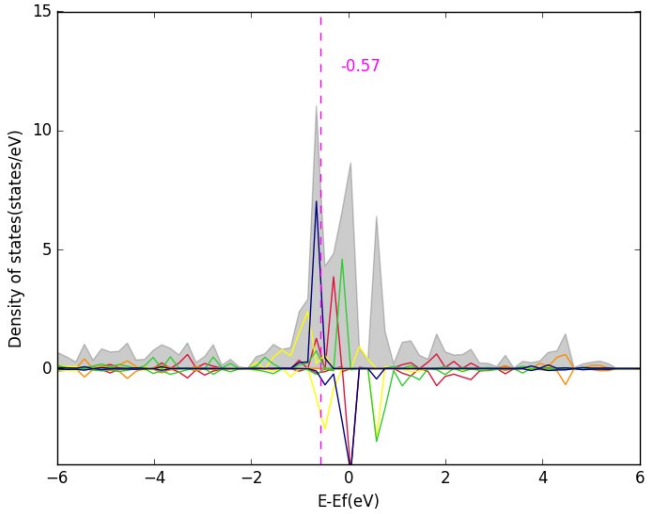

Ru-4N2v-CNT(8,8)

1/3

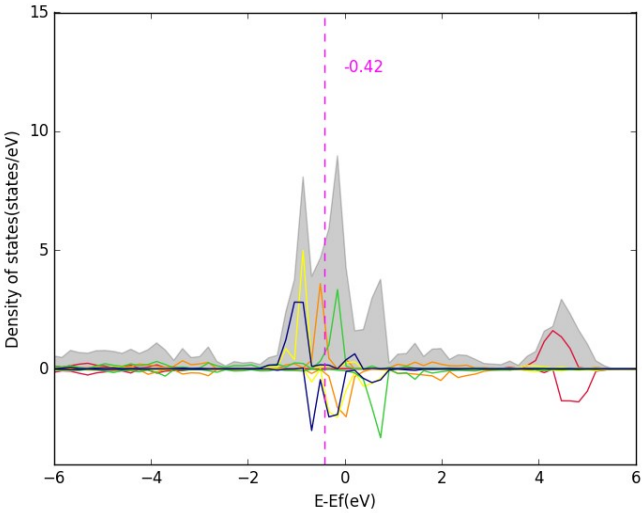

1/4

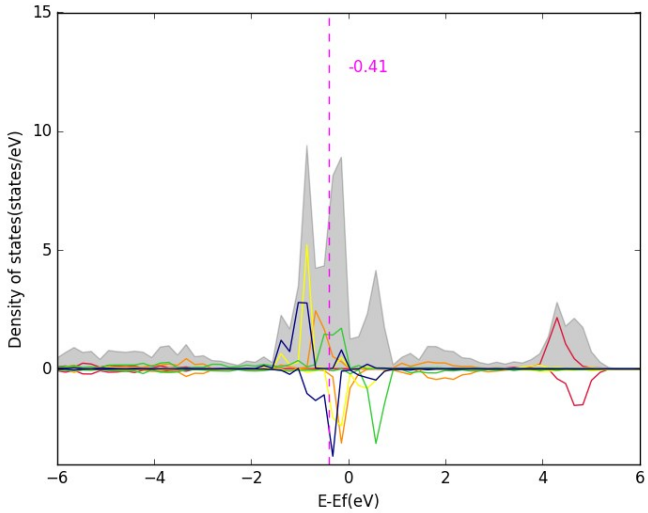

1/5

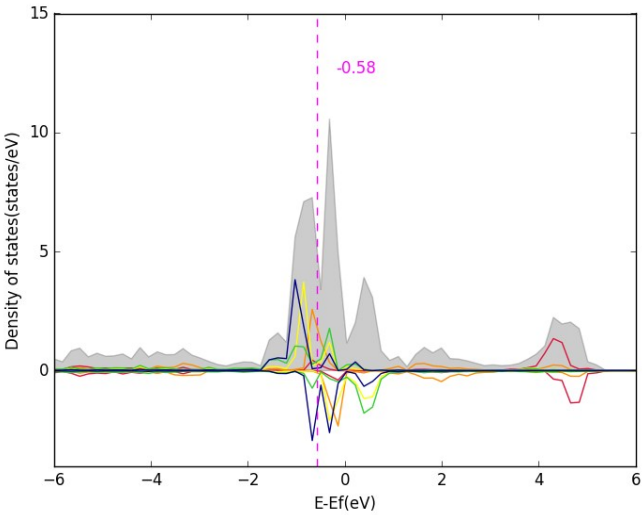

1/6

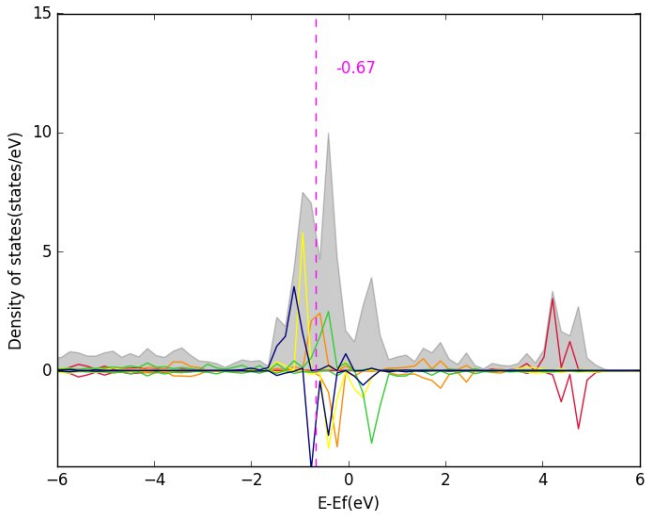

1/7

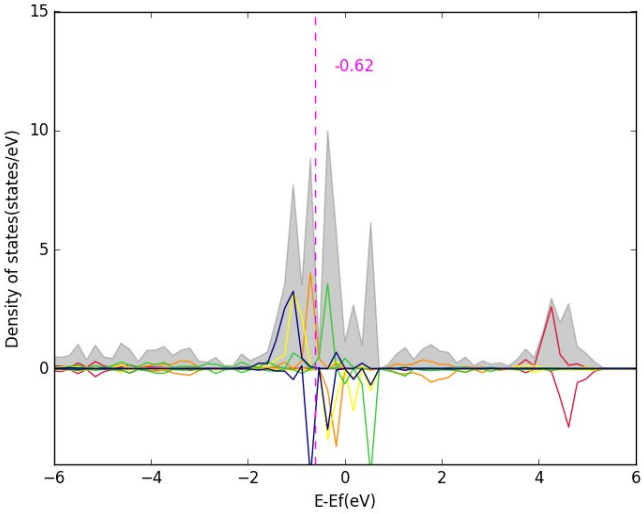

1/8

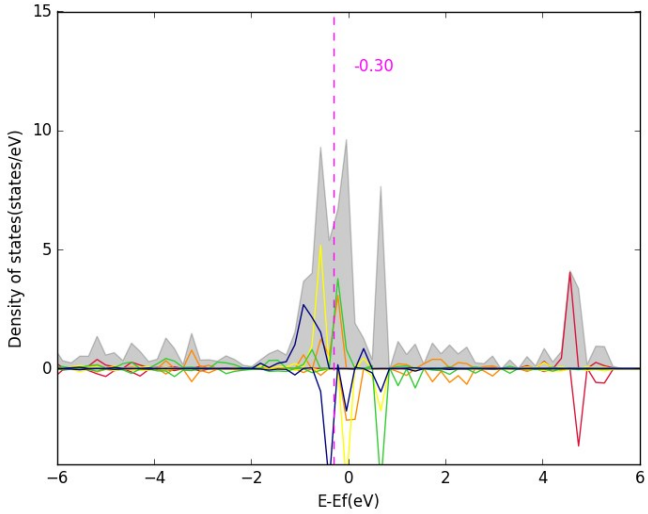

Ru-4N2v-CNT(10,10)

1/3

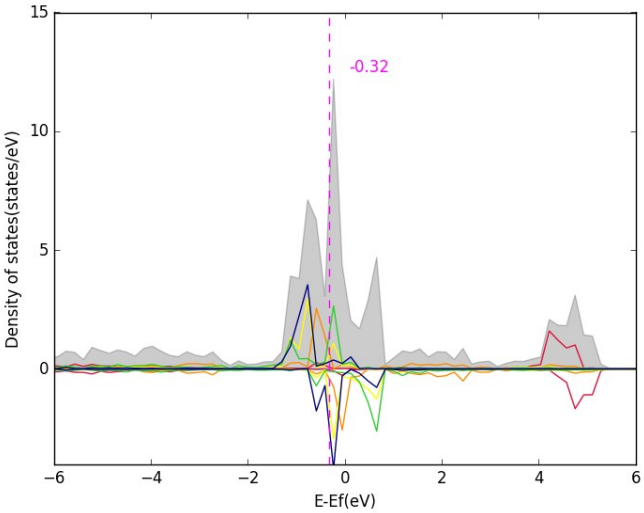

1/4

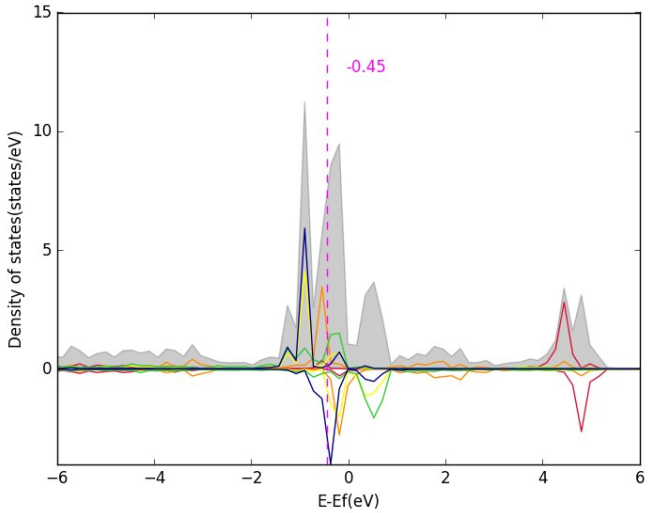

1/5

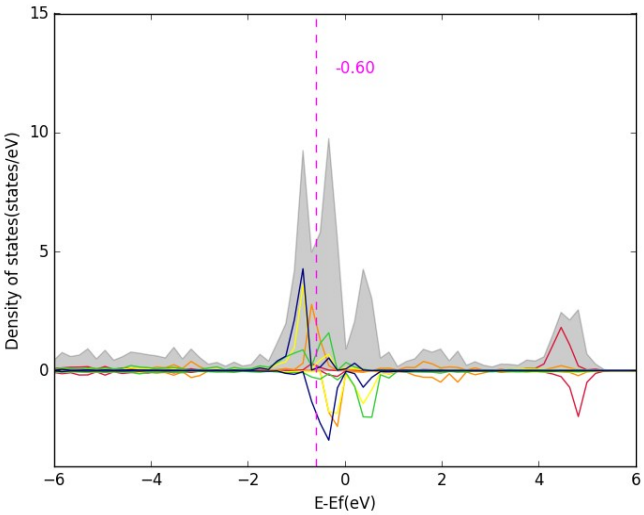

1/6

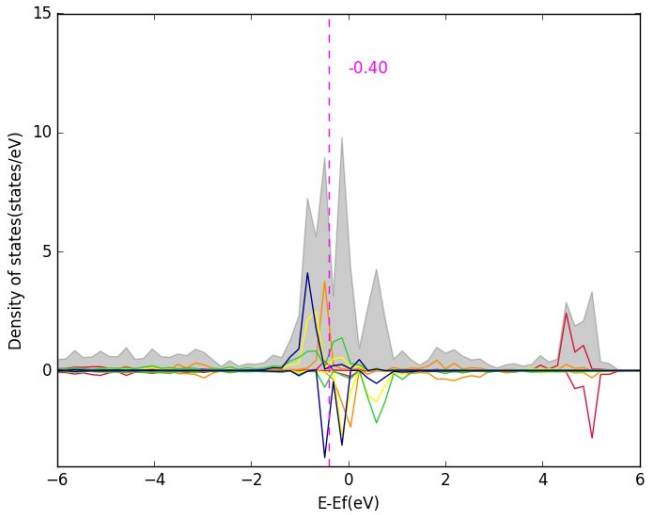

1/7

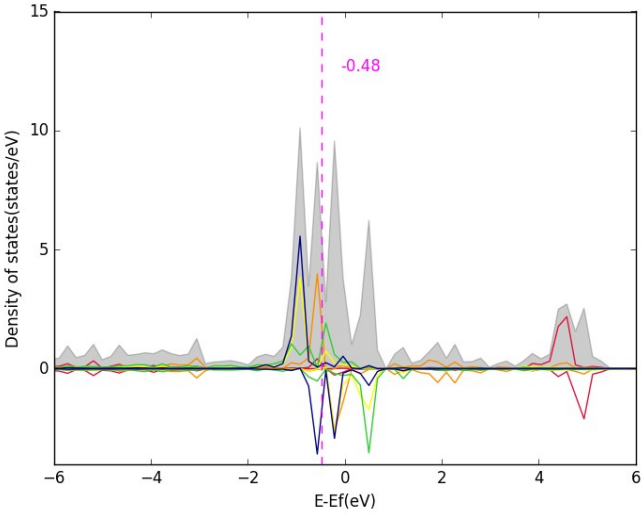

1/8

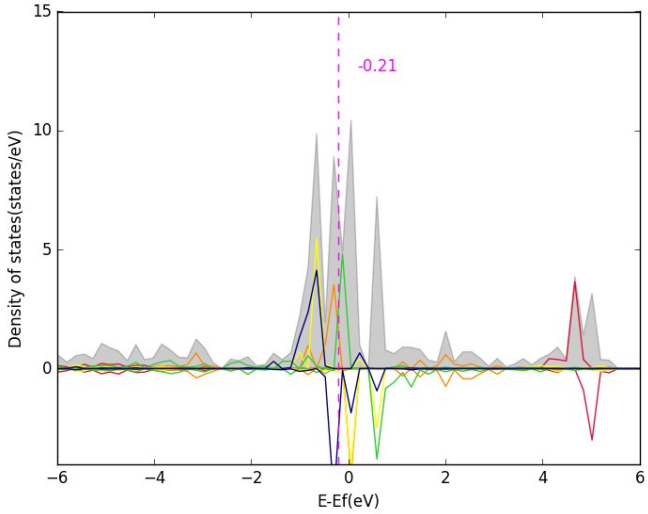

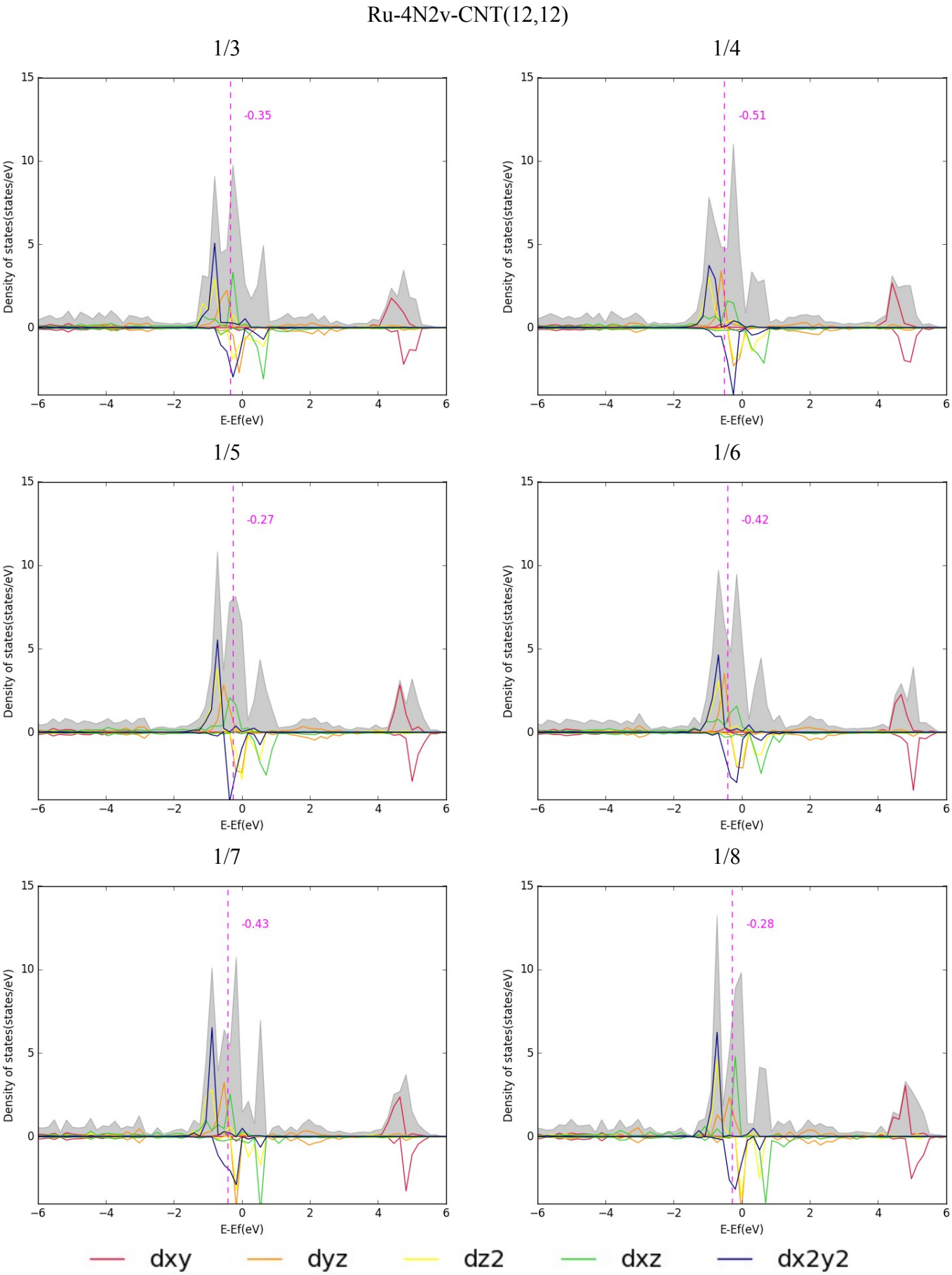

Figure S2. Partial density of states (PDOS) of Ru-4N2v-CNT(*n*,*n*) models, *n* = 5-8, 10 and 12. The d-band center of Ru is denoted in pink with total d-band in gray and the contribution of each d orbital in different color.

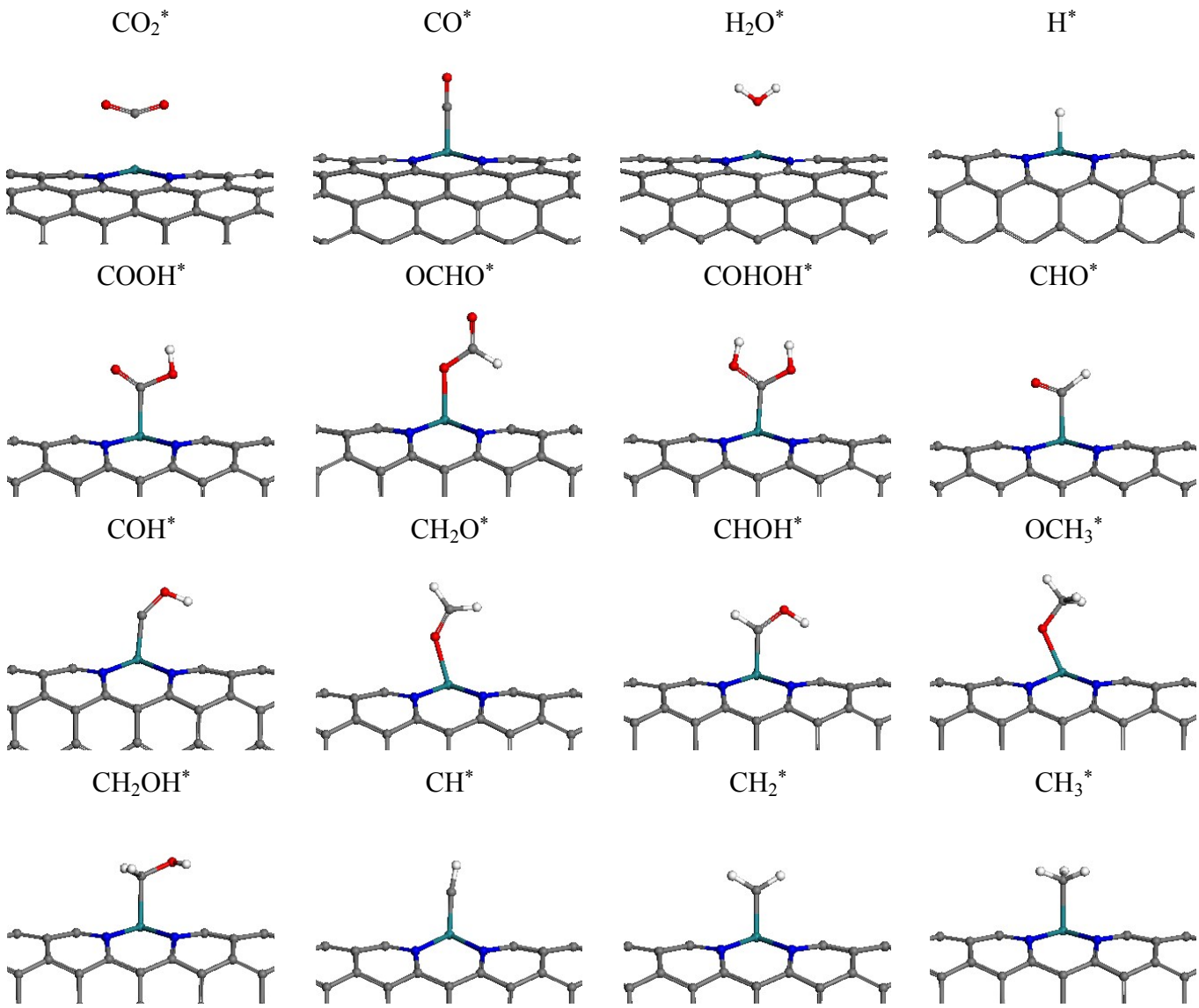

Figure S3. Schematic representations of the various adsorbent on Ru-4N2V-CNT models.

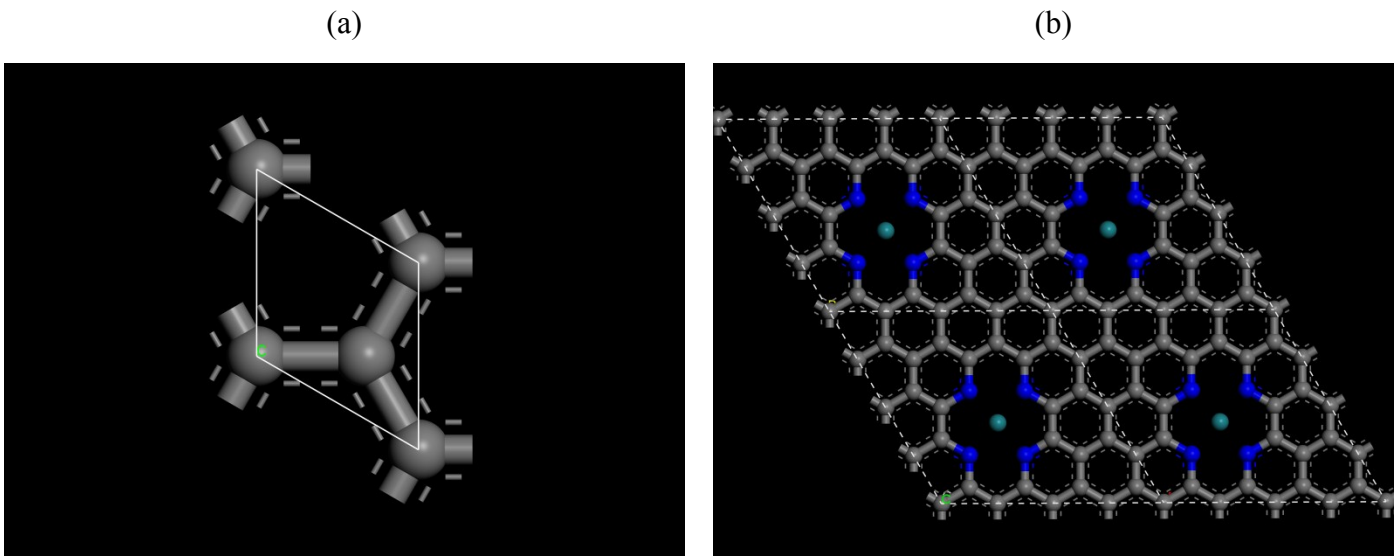

Figure S4. Schematic representations of (a) unit cell of graphene and (b) M-4N2v-graphene model at $\rho_s = 4$.

(5,5) (12,12)

Fe

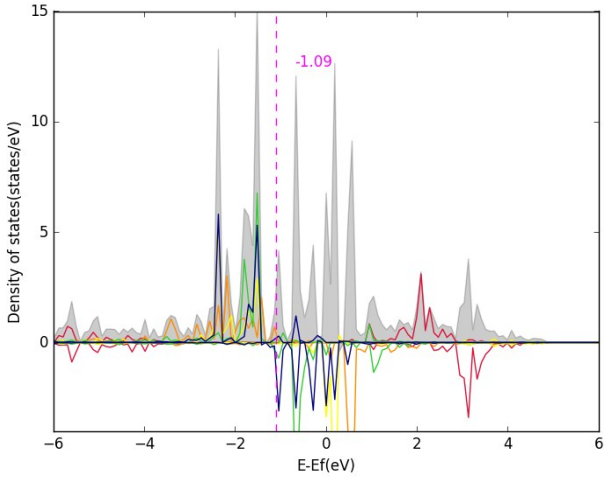

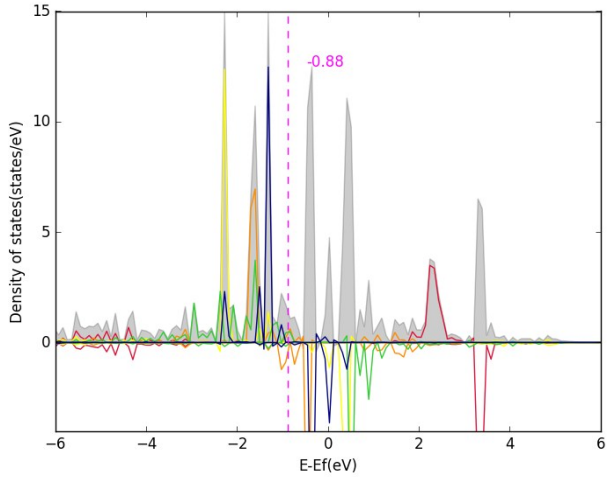

Ru

Os

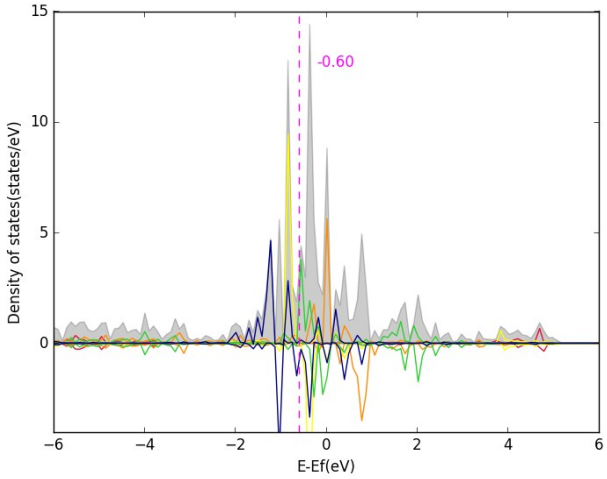

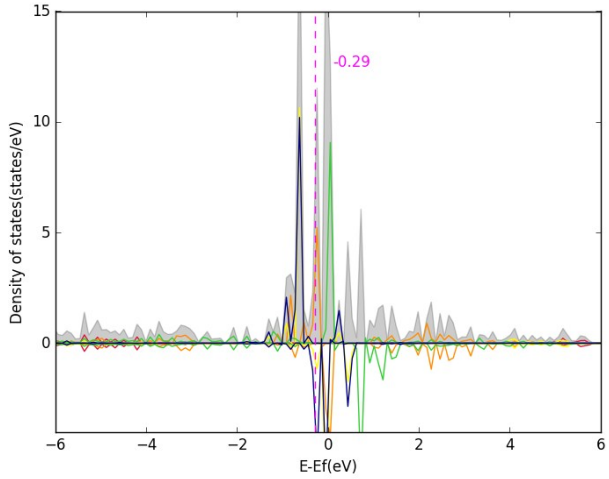

(5,5) (12,12)

Co

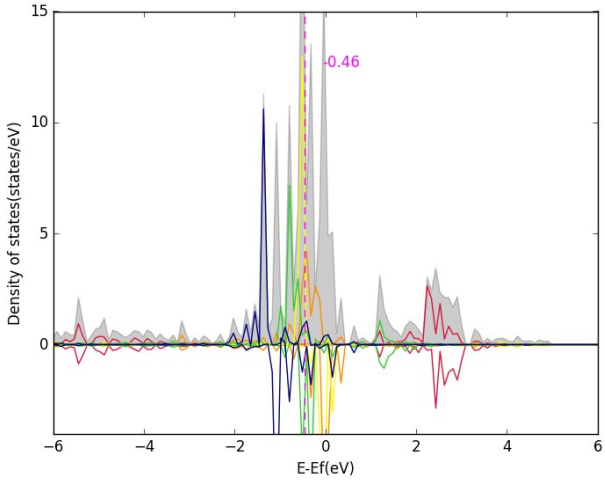

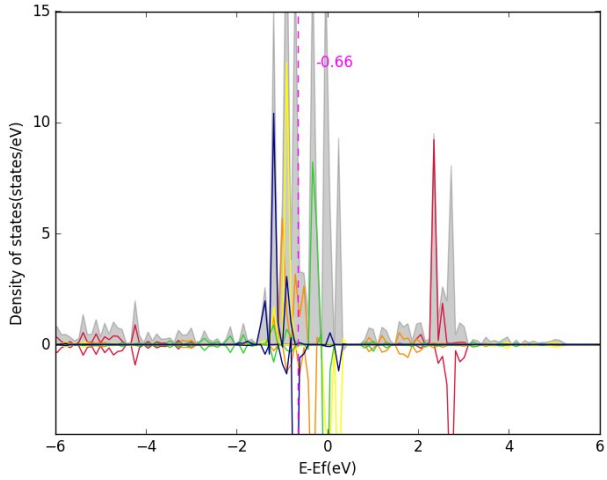

Rh

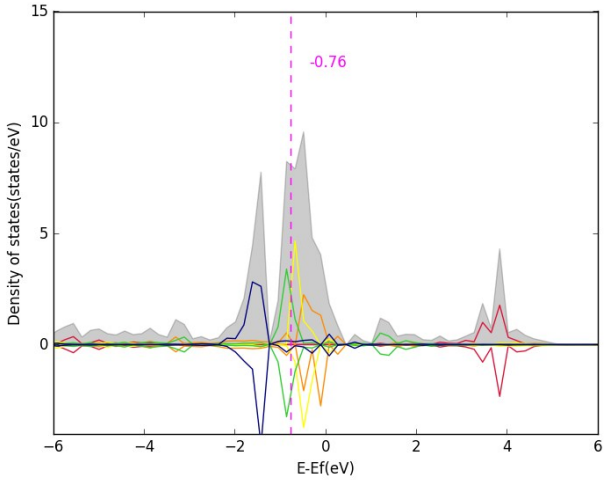

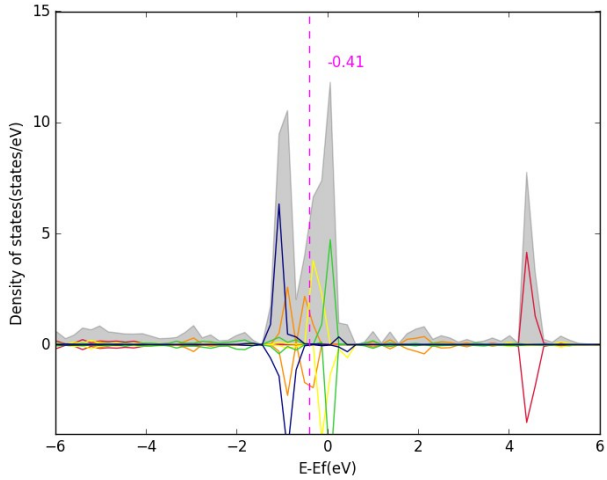

Ir

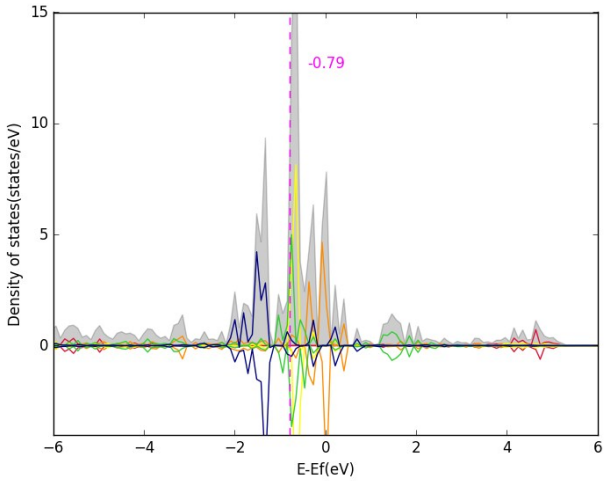

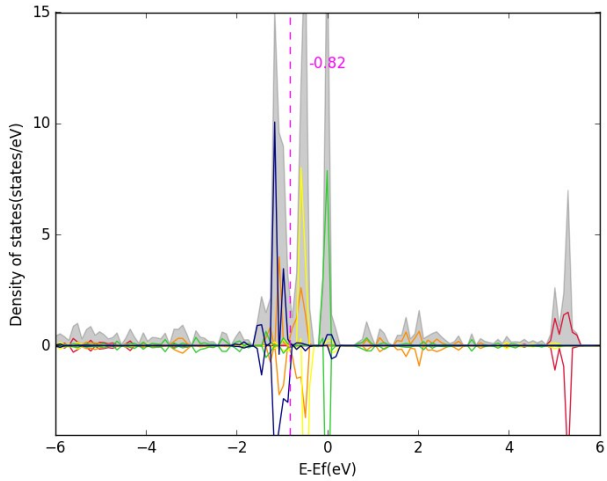

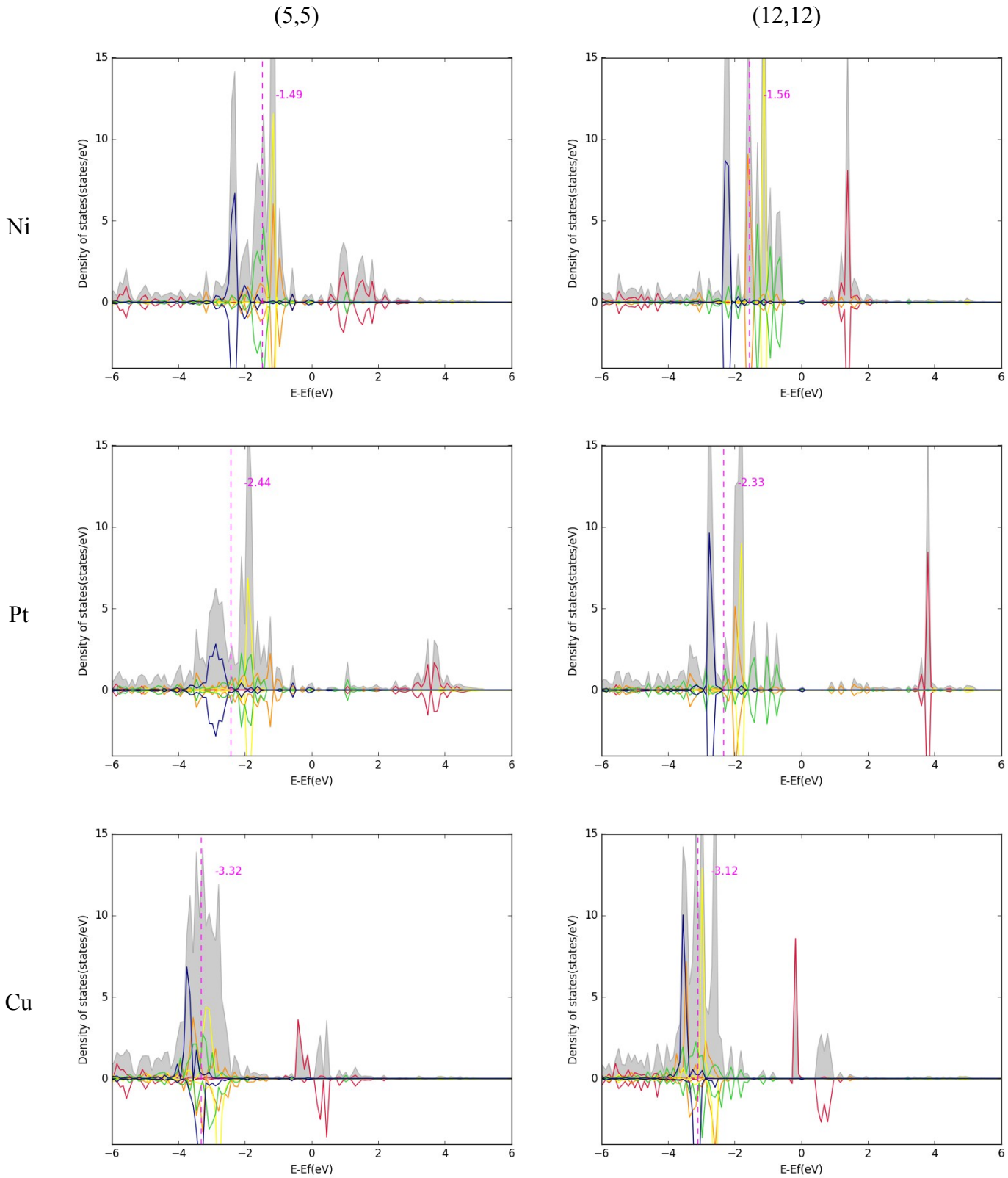

Figure S5. Partial density of states of TM-4N2v-CNT(*n*,*n*), *n* = 5 or 12, models.

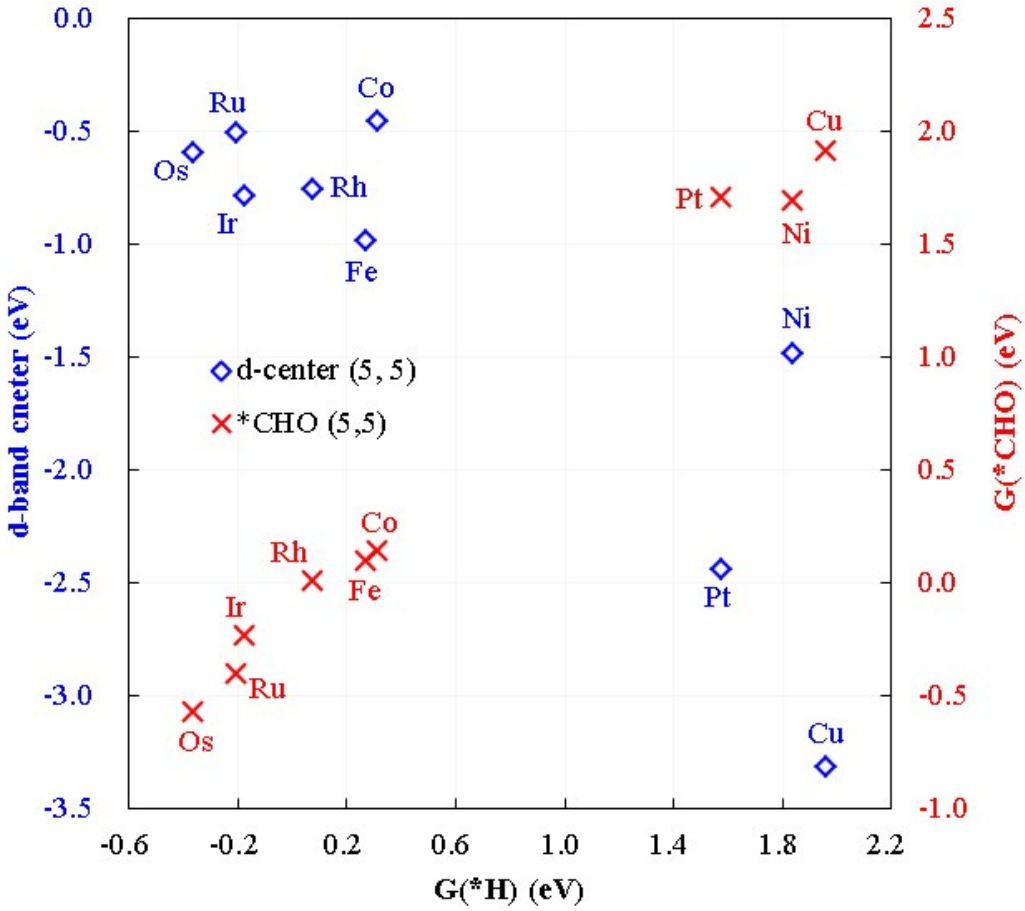

Figure S6. The scaling relations of d-band centers and G(*CHO) vs. G(*H) using TM-4N2v-CNT(5,5) models. Blue at the primary *y*-axis denotes the d-band centers and red at the secondary *y*-axis denotes G(*CHO).